Numerical analysis of the influence of inclination angle and wind on the heat losses of cavity receivers for solar thermal power towers

Robert Flesch[a], Hannes Stadler[a], Ralf Uhlig[b], Robert Pitz-Paal[c]

[a]*Institute of Solar Research, German Aerospace Center, Karl-Heinz-Beckurts Straße 13,D-52428 Jülich, Germany*
[b]*Institute of Solar Research, German Aerospace Center, Pfaffenwaldring 38-40, D-70569 Stuttgart, Germany*
[c]*Institute of Solar Research, German Aerospace Center, Linder Höhe, D-51147 Köln, Germany*

Abstract

The convective heat losses of cavity receivers for solar thermal power towers are of great importance for the overall efficiency of the whole system. However, the influence of wind on these losses has not been studied sufficiently for large scale cavity receivers with different inclination angles. In this present study the impact of head-on and side-on wind on large cavity receivers with inclination angles in the range of 0° (horizontal cavity) to 90° (vertical cavity) is analyzed numerically. The simulation results are compared to data published in literature. When no wind is present the losses decrease considerably with increasing inclination angle of the receiver. In case of a horizontal receiver wind does not have a huge impact on the losses: they remain constant on a high level. In case of an inclined cavity wind increases the heat losses significantly in most of the cases, although the highest absolute value of the losses occurs for the horizontal receiver exposed to head on wind. In some cases, when wind is flowing parallel to the aperture plane, a reduction of the heat losses is observed. The temperature distribution in the cavity is analyzed in order to explain the impact of wind on the heat losses. Wind in general causes a shrinking of the zone with uniform high temperature in the upper region of the cavity, whereas wind flowing parallel to the aperture plane additionally inhibits hot air from leaving the cavity and therefore leads

Email address: robert.flesch@dlr.de (Robert Flesch)

Preprint submitted to Solar Energy *May 22, 2014*

to an increased temperature in the lower zone.

Keywords: concentrating solar power, computational fluid dynamics, open cavity receiver, mixed convection, wind

1. Introduction

Concentrating solar power (CSP) plants are a promising option for future energy production. Since the produced heat can be easily stored, these power plants are capable of providing demand-oriented electricity from a renewable source. Different CSP technologies exist: parabolic trough systems, solar power tower systems and dish/engine systems. In solar power towers a large number of mirrors, the so-called heliostats, reflect the sunlight onto a receiver on the top of a central tower [1]. In the receiver, sunlight is absorbed and a fluid is heated, which can be used to produce electricity. In a dish system a single mirror tracks the sun and reflects it onto a receiver which is connected with the structure of the mirror.

Different designs for the receiver exist, one is the so-called cavity receiver. Here, the idea is to take benefit of the concept of a cavity in order to efficiently reduce the radiative losses. In technical designs radiative losses are eventually reduced to the same order of magnitude as the convective losses [2, 3]. Thus, it is very important to estimate the convective losses of cavity receivers in order to calculate the overall efficiency of the plant. In general, convective heat losses cannot be easily calculated due to the complexity of buoyant flows. A common approach to calculate these losses is to use correlations, making them dependent on the particular design. Due to the importance of an estimation of the losses, several studies focused on the analysis of convective heat losses of cavity receivers. Some of these studies are presented in the following structured by their approach: theoretical studies, experimental studies and finally studies using computational fluid dynamics (CFD) simulations.

1.1. Theoretical and early numerical studies

In the first studies on convective losses it was proposed to calculate the losses with correlations for a flat plate of the size of the aperture [4] or for all walls inside the cavity [5]. Later on, Eyler [6] performed an analysis of the flow inside a horizontal and an inclined cavity using a two-dimensional numerical code. The simulation results showed a stably-stratified region in

Nomenclature

Gr	Grashof number
Nu	Nusselt number
Re	Reynolds number
Ri	Richardson number
α	Angle of the wind direction
$\bar{\beta}$	Thermal expansion coefficient
$\bar{\nu}$	Kinematic viscosity at film temperature
ΔT	Temperature difference $T_{\text{wall}} - T_{\infty}$
λ	Local conductivity of the fluid
ν	Local kinematic viscosity of the fluid
ϕ	Inclination angle of the cavity receiver
ρ	Local density of the fluid
τ_{wall}	Wall shear stress
Θ	dimensionless temperature spread
$\bar{T}$	Film temperature
A_{Cavity}	Surface area of the inner cavity with the temperature T_{wall}
d	Inner diameter of the cavity
d_{ap}	Diameter of the receiver aperture
g	Acceleration of gravity
L	Inner length of the cavity receiver
T_{∞}	Temperature of the environment
T_{wall}	Temperature of the cavity receiver walls
u_{wind}	Wind velocity

the top of the cavity. Based on this upper zone inside the cavity Clausing [7–9] developed a numerical model, which can be used to estimate the losses for any cavity geometry. The cavity is divided into two zones by the horizontal layer which goes through the upper lip of the aperture (fig. 1). The fluid temperature in the upper zone, the so-called stagnant zone, is assumed to be equal to the wall temperature. For the walls in the lower zone, the so-called convective zone, standard correlations were used to calculate the heat flux from the walls into the convective zone. The layer between the zones is treated as wall as well. For the heat transfer through the aperture the velocity is calculated by assuming it is increasing linearly with the vertical

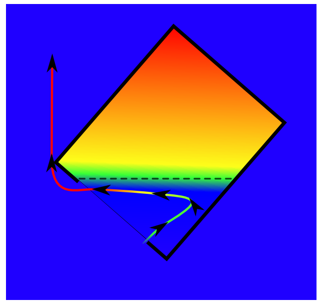

Figure 1: Sketch of the temperature distribution inside of an inclined cavity. The cavity is divided by the horizontal layer (dashed line) which goes through the upper lip of the aperture. The upper zone is called stagnant zone and the lower zone is the convective zone.

height of the aperture. For a cavity exposed to wind this velocity is combined with the wind velocity to an effective velocity through the aperture. As the heat transport is limited by the ability to transfer energy from the walls to the convective zone, the temperature inside the convective zone is close to the ambient temperature. Since wind increases only the energy transfer across the aperture, Clausing concluded that it has almost no influence on the convective losses.

1.2. Experimental studies

Kraabel [3] performed an experiment on convective heat losses using a cubical cavity with a Grashof number of $\mathrm{Gr} = 3 \cdot 10^{10}$. The cavity was mounted horizontally and only the losses caused by natural convection were analyzed. As the cavity was not placed inside a building, low wind velocity in front of the cavity could not be avoided, but no influence of the ambient wind on the convective losses was noted. In another experiment the losses of a receiver with a Grashof number $\mathrm{Gr} = 2.9 \cdot 10^{11}$ mounted on the top of a power tower were measured [2]. The receiver was heated up to $343\,^{\circ}\mathrm{C}$ and the total losses were estimated by measuring the flow rate of the heat transfer fluid and its temperature drop. The convective losses were calculated by subtracting the analytically calculated radiative and conductive losses. The receiver was exposed to different wind speeds up to Reynolds numbers of about $\mathrm{Re} = 7 \cdot 10^{5}$, but the influence of wind speed and wind direction were smaller than the accuracy of the experiment, again showing that under these boundary conditions the effect of wind is negligible.

In the following years research on the convective heat losses focused on smaller receivers used in dish applications. The losses of the cavity receiver used in the Shenandoah Project caused by natural and forced convection were analyzed in [10] and [11], respectively. The losses for wind speeds up to a Reynolds number of about $2.3 \cdot 10^5$, head-on and side-on wind for different receiver inclinations ($\phi = 0°...90°$) were measured [11]. The head-on wind as well as the side-on wind increased the losses of the receiver significantly in contrary to the findings described above. The author argued that this could be explained by the different length scale of the cavities. The ratio $\mathrm{Re}^2/\mathrm{Gr}$ was about one order of magnitude higher in his experiment compared to the cavities analyzed in the other studies. This ratio, also known as the inverse Richardson number Ri^{-1}, represents the influence of forced convection related to natural convection.

The influence of low wind speed (up to $\mathrm{Re} = 0.6 \cdot 10^5$, head-on and side-on) on the losses of cavity receivers for dishes with different inclination angles ($\phi = 0..90°$) was analyzed by Prakash et al. [12]. The experiment showed that with increasing inclination of the receiver, wind has a higher impact on the heat losses. However, the highest absolute losses were measured for the receiver with no inclination and head-on wind. Side-on wind for the horizontal receiver even leads to a decreased heat-loss, which was explained by an obstruction of the air leaving the receiver due to the wind.

1.3. CFD simulations

With increasing computational power in the past years it is nowadays possible to use CFD models to predict the losses of cavity receivers. The CESA-1 receiver of the Plataforma Solar de Almeria was simulated under windy conditions [13]. As expected from the previous discussion, the temperature inside the cavity did not change with increasing wind speed. However, the losses increased slightly, which was explained by an enhanced heat transfer at the cavity walls. Another CFD simulation carried out for a face-down cavity receiver for solar-reforming showed a substantial increase of the convective losses for higher wind speeds [14].

Altogether the influence of wind on the convective heat loss of cavity receivers has been analyzed in several studies, but the analyses came to different conclusions about the influence of wind. As mentioned above, the differences in the results were accounted to the different sizes of the cavities. Some of the cavity receivers were smaller because they were designed for dish applications whereas the cavity receivers for solar towers are substantially larger. Therefore, the influence of wind compared to the influence of the buoyancy was different for the analyzed cavity receivers, which can be expressed by the ratio $\mathrm{Re}^2/\mathrm{Gr}$ [11]. Hence, there is still a high uncertainty concerning influence of wind on large cavity receivers for solar power towers, since a systematic analysis of the influence of wind on cavity receivers with different inclination has not been performed yet. The purpose of this study is to perform such a systematic analysis by using CFD simulations.

2. Numerical model and setup

Since the purpose of this study is a general analysis of the influence of wind on the convective losses, an isolated axisymmetric cavity in a wind tunnel like environment was simulated. The simulations were carried out for the following dimensionless parameters

$$\mathrm{Gr} = \frac{\bar{\beta}\,\Delta T g d^3}{\bar{\nu}^2} = 2.9 \cdot 10^{10} \tag{1}$$

$$\Theta = \frac{T_{\mathrm{wall}} - T_\infty}{\bar{T}} = 1.085 \tag{2}$$

with the thermal expansion coefficient β, the inner diameter of the cavity d, the temperature difference between the walls of the cavity and the ambient air ΔT, the acceleration of gravity g and the kinematic viscosity ν. The fluid properties for the dimensionless numbers are evaluated at the film temperature

$$\bar{T} = 0.5 \cdot (T_{\mathrm{wall}} + T_\infty)\,. \tag{3}$$

The simulations were performed for different wind velocities u_{wind} up to a Reynolds number of

$$\mathrm{Re} = \frac{u_{\mathrm{wind}} d}{\bar{\nu}} = 3.4 \cdot 10^5\,. \tag{4}$$

The wind velocity was assumed to be constant and a steady state in-flow condition was used.

A sketch of the cavity geometry and the surrounding, illustrating the dimensions, is shown in fig. 2. The cavity has an aperture $d_{\mathrm{ap}} = 0.6d$ and an inner length $L = 1.08d$. In the simulation the inner cylindrical wall and the end of the cavity are kept at a constant uniform temperature. All other walls are assumed to be adiabatic, because only the convective losses from

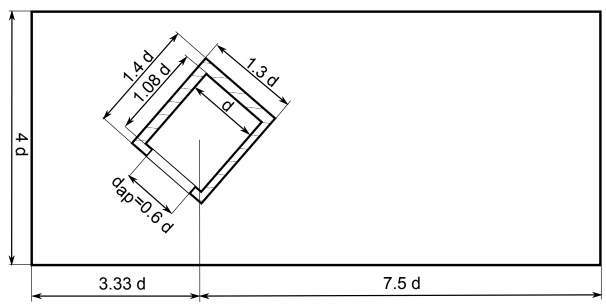

Figure 2: Sketch of the Cavity inside the wind tunnel like surrounding

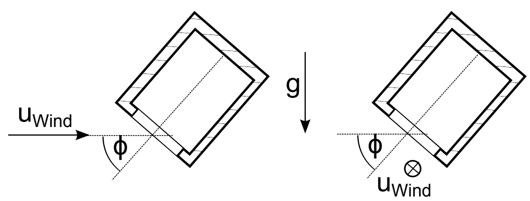

Figure 3: Definition inclination angle (ϕ) of the cavity. On the left the head-on ($\alpha = 0°$) and on the right the side-on ($\alpha = 90°$) wind case is shown.

the inner cavity are in the focus of this study. The convective heat losses of the inner cavity walls

$$\dot{Q} = \lambda \cdot \frac{dT}{dn} \tag{5}$$

is calculated using the surface normal gradient of the Temperature $\frac{dT}{dn}$ and the local conductivity of the fluid λ. Using the heat losses the dimensionless Nusselt number is obtained with

$$\mathrm{Nu} = \frac{\dot{Q} \cdot d}{\Delta T A_{\mathrm{Cavity}} \cdot \bar{\lambda}} \tag{6}$$

Two different wind directions were simulated: head-on wind ($\alpha = 0°$) and side-on wind ($\alpha = 90°$), each for a cavity with an inclination angle ϕ of 0°, 30°, 60° and 90°. The angle definitions are shown in fig. 3. The angle of the wind direction and the cavity inclination angle can be varied independently.

The full set of equations, that is the continuity equation, Navier-Stokes equation and energy equation were solved using the CFD code OpenFOAM 2.2.0 [15] with variable fluid properties and perfect gas behavior. For pressure-velocity coupling the SIMPLE scheme was used and all derivatives were discretized with second order schemes. The flow in the cavity is slightly unstable as are many buoyancy driven flows. In order to obtain reliable results, an unsteady RANS method is applied [16]. Turbulence is modeled using the k-ω-SST turbulence model.

A mesh consisting of hexahedral elements was created for the geometry. The dimensionless wall distance $y^+ = \frac{y \cdot \sqrt{\tau_{\text{wall}}}}{\nu \cdot \sqrt{\rho}}$ for every wall participating in the heat exchange was designed to be on the order of one. A two-step mesh convergence study using three different meshes was performed by increasing the number of elements in each direction by a factor of about 1.3. For a horizontal cavity ($\phi = 0°$) at the highest Reynolds number the resulting Nusselt number on the finest mesh containing about 4.2 million elements differs less than one percent compared to the next coarser mesh. Thus, the finest refinement level was used for all the calculations.

3. Results

3.1. Integral results

Figure 4 shows the Nusselt number for the convective heat losses versus the ratio $\mathrm{Re}^2/\mathrm{Gr}$ for head-on wind ($\alpha = 0°$). A large value of $\mathrm{Re}^2/\mathrm{Gr}$ means that the influence of buoyancy can be neglected. Additionally to the simulation results indicated by the markers, the heat losses as predicted by the model proposed by Clausing [8] are shown with lines. This model was chosen as comparison because predictions based on this model have been proven to give good results in case of natural convection for a huge range of different geometries [17]. The model includes the influence of wind, however, it predicts that its influence is small. For a horizontal cavity receiver the model predicts a slight increase of the losses for small wind velocities. For higher velocities the losses remain almost constant. With increasing cavity inclination the losses become more and more independent of the wind velocity. In case of a face-down receiver ($\phi = 90°$) this model predicts the losses to be constantly zero.

In case of natural convection ($\mathrm{Re}^2/\mathrm{Gr} = 0$) the simulation results, indicated by the markers, match the prediction of the Clausing model well when looking at the relative deviation except for the case of a face-down receiver: in contrast to the prediction of the Clausing model the simulations show that a face-down receiver has low convection losses even without wind.

For the case of a horizontal receiver exposed to head-on wind the simulation results also agree with the prediction of the model. However, for cavities

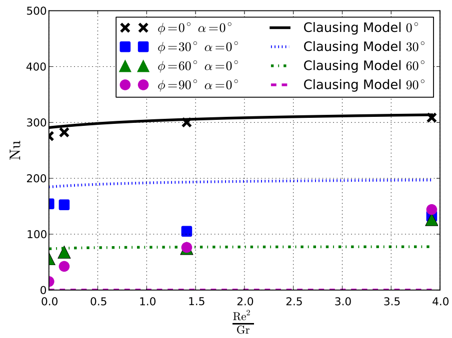

Figure 4: Nusselt number shown as a function of $\mathrm{Re}^2/\mathrm{Gr}$ for different receiver inclinations with head-on wind ($\alpha = 0°$). Besides the simulation results, the results of the Clausing model [8] are shown.

with higher inclination angles ($\phi > 0°$) the simulation results deviate from the losses predicted by the model. In contrast to the model, the influence of wind increases in the simulation for cavity receivers with higher inclination angles. For a cavity receiver with an inclination angle of $\phi = 60°$ the losses at the highest wind speed exceed the losses of the no-wind case by a factor of three, whereas the face down receiver has about 9.5 times higher losses. The results for the cavity receiver with a 30° inclination angle differ from the other simulated cases. The losses are reduced at low wind speeds. After reaching a minimum at medium velocity case they start increasing again.

The results for the side-on wind ($\alpha = 90°$) case are shown in fig. 5. As the Clausing model does not include the influence of the wind direction, the results for the model are the same as in in the head-on wind case shown in fig. 4. The simulation results, however, differ from the head-on wind case and, accordingly, they deviate from the results of the model as well. For the horizontal receiver small wind velocities lead to slightly increased losses. But once again the medium wind velocity causes a reduction of the losses before they increase again for the highest velocity case. The same trend occurs for the 30° inclined cavity, although the reduction is not as distinct as for the horizontal cavity. For the case of the cavity receiver with an inclination angle of 60° no reduction is observed in the simulations. Results for the face down receiver are the same as in the head-on wind case.

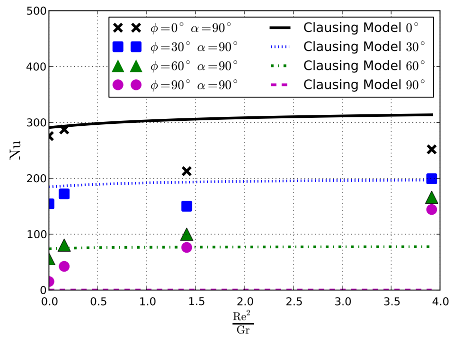

Figure 5: Nusselt number shown as a function of $\mathrm{Re}^2/\mathrm{Gr}$ for different receiver inclinations with side-on wind. Besides the simulation results, the results of the Clausing model [8] are shown.

3.2. Detailed analysis of the flow structure

An analysis of the temperature and velocity field inside the cavity receiver gives an insight into the influence of wind. Figure 6 shows the combined vector and temperature plot of a vertical slice through the center of the cavity for the case of $\mathrm{Re}^2/\mathrm{Gr} = 1.4$. The cavity design protects the inner fluid from the wind outside, which results in much smaller velocities inside. The temperature underneath the horizontal plane that goes through the upper lip of the aperture is close to the ambient temperature, whereas the temperature above this layer is significantly higher. However, in this case it is not equal to the wall temperature as assumed by Clausing [8].

For further analysis, the temperature distribution inside the cavity is reduced to a mean temperature profile along the vertical axis (black line in fig. 6). For this the temperature along a horizontal line in the central vertical plane of the inner cavity (dashed line in fig. 6) is averaged. These mean temperature profiles for a horizontal cavity are shown in fig. 7. This plot can be used to analyze the influence of wind on the temperature distribution inside the cavity. The position of the horizontal layer through the upper lip of the aperture is illustrated with the horizontal thin dashed line. The two zones described above can be seen as well: the increased temperature in the upper region and the region with the temperature close to ambient temperature below. By comparing the profiles for the different velocities it can be seen that wind does not have a significant impact on the temperature distribution inside a horizontal cavity. This results in almost unchanged losses compared

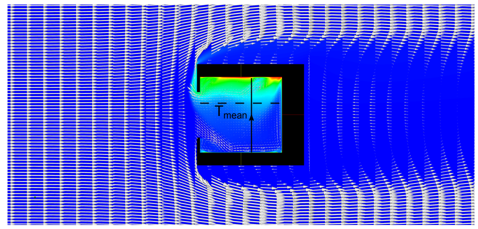

Figure 6: Combined temperature and velocity plot for the horizontal cavity ($\phi = 0°$) and head-on ($\alpha = 0°$) wind with $\mathrm{Re}^2/\mathrm{Gr} = 1.4$. The mean temperature profiles are obtained by calculating the mean temperature for each horizontal (dashed) line along the vertical axis inside the cavity.

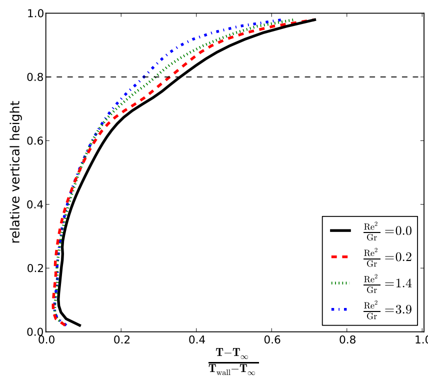

Figure 7: Mean dimensionless temperature profile along horizontal lines inside the cavity as a function of the relative vertical height for the case $\phi = 0°$ and $\alpha = 0°$. Wind does not change the mean temperature profile significantly.

to the natural convection case and is in good agreement with the analysis of Clausing [8].

For the case of a cavity with an inclination of $\phi = 30°$ things are different (fig. 8). In case of natural convection and lowest wind speed the air temperature in the upper third of the cavity equals the wall temperature. In the middle is a transition zone, where the temperature decreases almost linearly from wall temperature to nearly ambient temperature. The horizontal layer through the upper lip of the aperture is located in this zone. In the lower third the temperature is close to ambient temperature. The temperature in this lowest zone increases only slightly from no-wind case to the case of the lowest wind speed, whereas it is significantly higher in the two cases with higher wind speeds. At the same time, the size of the region in which the

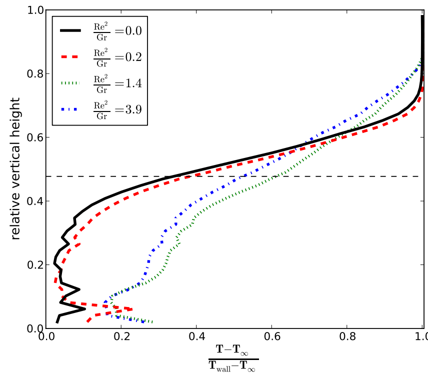

Figure 8: Mean dimensionless temperature profile along horizontal lines inside the cavity as a function of the relative vertical height for the case $\phi = 30°$ and $\alpha = 0°$. Higher wind velocities lead to an increased temperature in lower region of the cavity.

temperature equals the wall temperature shrinks.

The same two effects occur for the receiver with the inclination angle $\phi = 60°$, but in this case the size of the zone with constant temperature is larger than the other two zones as it can be seen in fig. 9. Additionally, in this case wind has a more distinct influence on the zones: with increasing wind speed the size of the zone with constant temperature shrinks, whereas the size of the transition zone increases. The mean temperature distribution

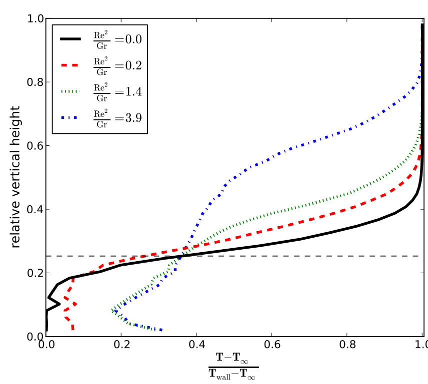

Figure 9: Mean dimensionless temperature profile along horizontal lines inside the cavity as a function of the relative vertical height for the case $\phi = 60°$ and $\alpha = 0°$. The increased temperature in the lower zone comes along with a decreased size of the upper zone.

inside the vertical cavity does not differ very much from the $\phi = 60°$ case (fig.

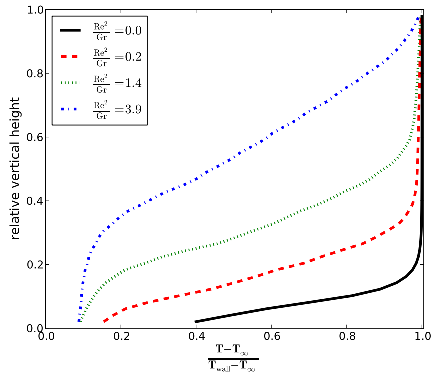

Figure 10: Mean dimensionless temperature profile along horizontal lines inside the cavity as a function of the relative vertical height for the case $\phi = 90°$ and $\alpha = 0°$. Wind reduces the mean temperatures everywhere in the cavity.

10). In this case the size of the constant temperature zone extends almost throughout the entire cavity in case of natural convection, but its size shrinks distinctly when wind is present.

As it was already shown before, the influence of side-on wind is quite different, but once again the temperature distribution inside the cavity gives a deeper insight. Low wind speeds coming from the side for the case of a horizontal cavity result in a higher temperature inside the convective zone compared to the case of natural convection as shown in fig. 11. For the highest wind velocity analyzed in this study with $\mathrm{Re}^2/\mathrm{Gr} = 3.9$ the mean temperatures inside the cavity are reduced again compared to the temperature profile for the case $\mathrm{Re}^2/\mathrm{Gr} = 1.4$. But they are is still higher than in the no-wind case, which means that the respective heat flux from the walls into the cavity is lower. Therefore, the losses are reduced compared to the natural convection case.

The side-on wind for cavities with higher inclination leads to an increased temperature in the convective zone as well, as shown exemplary for the cavity with an inclination of 60° in fig. 12. But at the same time it forces the layer between the two zones to move upward, which, on the contrary, causes higher losses.

Comparing all the plots for the mean temperature profiles of the cavities in case of natural convection one noticeable feature appears: throughout all inclination angles the dimensionless temperature at the height of the upper lip of the aperture is a constant value of $(T - T_\infty)/(T_{\mathrm{wall}} - T_\infty) \approx 0.37$.

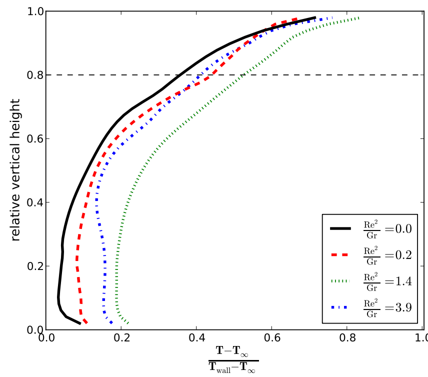

Figure 11: Mean dimensionless temperature profile along horizontal lines inside the cavity as a function of the relative vertical height for the case $\phi = 0°$ and $\alpha = 90°$. Side-on wind results in higher mean temperatures almost everywhere inside the cavity. After reaching a maximum for $\mathrm{Re}^2/\mathrm{Gr} = 1.4$ the mean temperatures along the relative cavity height drop again for the highest simulated velocity.

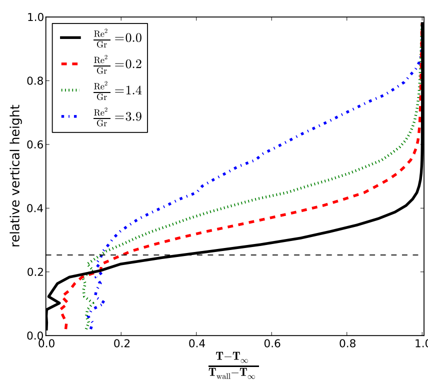

Figure 12: Mean dimensionless temperature profile along horizontal lines inside the cavity as a function of the relative vertical height for the case $\phi = 60°$ and $\alpha = 90°$. For high inclined cavities wind reduces the size of the upper zone with constant temperature significantly.

4. Discussion

The simulated mean temperature profile showed three different zones inside the cavity: In the top a zone where the temperature is equal to the wall temperature, at the bottom a zone where the temperature is close to ambient temperature and in between a transitional zone where the temperature decreases almost linearly from wall temperature to ambient temperature. For the horizontal cavity receivers the uppermost zone is missing, because the region above the upper lip of the aperture is too small. In Clausing's [8] model these three zones are merged into two zones: the convective zone and the stagnant zone. The transition zone is neglected. This is a good approximation in the natural convection cases. Thus, the losses predicted by the model and the simulations match quite well. When the cavity is exposed to wind, however, the simulations indicate a shrinking of the upper zone with constant temperature and an increasing transition zone, especially for the inclined cavity receivers. This is probably due to the fragility of the thermal stratification, which is disturbed by the slightly increased velocities inside the cavity when wind is present. When the upper zone is shrinking, some parts of the walls, which are in the constant temperature zone in the natural convection case, now contribute to the losses. Hence the losses increase. In the Clausing model the position of the layer between the stagnant and the convective zone is not influenced by wind and therefore, this effect does not occur in the model.

In some cases a temperature rise in the convective zone can be observed as mentioned in section 3. This is believed to be caused by wind flowing parallel to the aperture plane. The external flow inhibits hot air to flow through the aperture. The hot air is redirected back to the convective zone, causing an increased temperature in this zone. As a result of the increased temperature level the heat flux from the walls into the convective zone is reduced. This is associated with decreasing heat losses. The same effect can be explained by analyzing the heat transfer across the aperture out of the cavity. The heat flux out of the cavity must be equal to the heat flux from the walls into the cavity. Wind changes the energy transport across the aperture: the flow parallel to the aperture results in a much higher resistance for this energy flux. As a consequence the temperature inside the cavity must increase. However, with increasing wind speed the resistance is reduced again due to an enhanced energy transfer across the aperture. This leads to a decreasing temperature in the stagnant zone in case of the highest investigated velocity

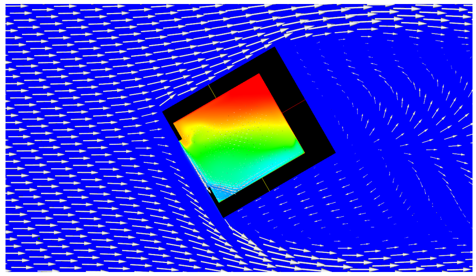

(a) View on the whole cavity

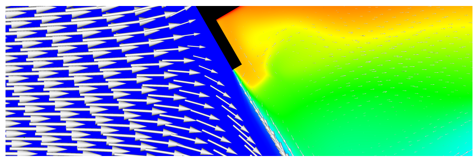

(b) Close up of the aperture

Figure 13: Combined temperature and velocity plot for the cavity with an inclination angle $\phi = 30°$ and head-on ($\alpha = 0°$) wind with $\mathrm{Re}^2/\mathrm{Gr} = 1.4$. The air is redirected by the front cover of the cavity and flows parallel to the aperture plane.

(see fig. 11) and an increasing convective heat loss. The flow parallel to the aperture occurs in the side-on wind cases, but as well in the head-on wind ($\alpha = 0°$) cases with inclined cavities as shown in fig. 13. In the latter cases the air is redirected by the front cover of the cavity.

In most of the cases both effects occur simultaneously: wind results on the one hand in a shrinking stagnant zone and on the other hand in an increased temperature inside the convective zone. Depending on which effect is dominant, wind leads to increasing or decreasing heat losses with rising wind speed. In the cases, in which wind leads to reduced losses, the losses are minimal for wind speeds around $\mathrm{Re}^2/\mathrm{Gr} = 1.4$. In this case wind and buoyancy have almost the same influence on the flow. For higher wind speeds, wind becomes dominant and the losses start to increase again. However, even for the case of the highest simulated wind speed the heat losses are still a mixed convection problem: otherwise the convective heat losses would be the same for the cavities with different inclination angles exposed to side-on wind.

The results for a horizontal receiver are consistent with the observation described in [2, 3]. It is likely that the slight changes of the losses cannot be measured in a receiver used in a power tower. For inclined large cavities used in power towers no experiments have been performed yet. However, experimental data exist for smaller cavities used in dish systems. Increasing losses with rising wind speed are reported in [11, 12]. This is consistent with the results of the present simulation. A reducing effect of wind on the losses was not observed by Ma [11], but his experiment was performed for relatively high wind velocities. Prakash et al. [12], who focused on small wind velocities, described a reduction of the losses for a horizontal cavity. In order to compare the results of the present simulations for the large cavity to the results of the smaller cavities it is interesting to take a closer look at the ratio

$$\frac{Re^2}{Gr} = \frac{u_{\text{wind}}^2}{\beta \Delta T g d} \propto \frac{u_{\text{wind}}^2}{d} \,. \tag{7}$$

As mentioned above, this ratio represents the influence wind to buoyant effects on the heat losses. In order to keep this ratio and therefore the balance of wind to buoyant effects constant, wind speed must be decreased for smaller cavities. This might be an explanation why the reduction occurs for smaller wind speeds in case of a smaller cavity. In the experiment performed by Prakash et al [12] a reduction was only observed for the horizontal cavity and side-on wind, but the cavity used in that experiment in contrast to the present cavity had a ratio d_{ap}/d of approximately one so that apparently the effect show in fig. 13 does n5ot occur. This leads to the conclusion that the reduction of the losses by wind might depend strongly on the actual geometry of the cavity. It should be mentioned, that the absolute values of the Grashof and the Reynolds number are relevant to the losses and therefore the results are not fully transformable, but the comparison gives more confidence in this special phenomenon occurring in the simulation.

5. Conclusion and Outlook

The influence of head-on wind ($\alpha = 0°$) and side-on wind ($\alpha = 90°$) on cavity receivers with different inclination angles in the range of 0° to 90° has been analyzed numerically. The results were compared to the Clausing model described in [8]. When no wind is present the Clausing model and the simulation results match very well. Additionally, for the case of a horizontal cavity and head-on wind model and simulation give almost the same prediction for the convective heat losses. Both, simulation and model, show that wind has only a small influence on the losses of horizontal cavity receivers, although they give different results in case of the side-on wind. For cavity receivers with higher inclination angles simulations show in most of the cases a distinct increase of the losses, which is in contrast to the predictions of the Clausing model. Mean profiles of the temperature distribution inside the cavity were used to show that the stagnant zone shrinks with increasing wind speed, which results in higher losses. Predictions of a model could be improved by including this effect. In some cases a reduction of the heat losses with increasing wind speed was observed. This effect was explained by wind flowing parallel to the aperture plane, which inhibits hot air from leaving: a temperature raise was noted in the mean temperature profiles. It is likely that this effect depends strongly on the geometry of the cavity. However, in following investigations it might be an interesting option for a reduction method of the losses: the receiver should be designed in a way that wind is redirected to flow parallel to the aperture plane.

In accordance with the previous numerical analyses a steady state inflow condition was used, in order to obtain comparable results. However, it might be interesting to study the influence of a time variable wind speed and direction as the wind conditions in front of a receiver change as well.

The obtained results from the simulation were discussed in the context of available experimental results. The results are in accordance with published results for horizontal cavities, where data is available for power tower receivers. A scaling approach was introduced to compare simulation results of the large cavity to experimental data of small cavities which were designed for dish systems. However, an experimental analysis of large scale cavity receivers for power towers should be pursued.

Appendix A. Acknowledgment

This work was carried out with financial support from the Ministry of Innovation, Science and Research of the State of North Rhine-Westphalia (MIWF NRW), Germany under contract 323-2010-006 (Start-SF).

References

[1] M. Romero, R. Buck, J. E. Pacheco, An Update on Solar Central Receiver Systems, Projects, and Technologies, Journal of Solar Energy Engineering 124 (2002) 98–108.

[2] R. K. McMordie, Convection Heat-Loss From A Cavity Receiver, Journal of Solar Energy Engineering-Transactions of the ASME 106 (1984) 98–100.

[3] J. Kraabel, An Experimental Investigation of the Natural Convection from a Side-Facing Cubical Cavity, in: Y. Mori, W. J. Yang, American Society of Mechanical Engineers, Japan Society of Mechanical Engineers, ASME-JSME Thermal Engineering Joint Conference (Eds.), ASME-JSME Thermal Engineering Joint Conference: Proceedings, volume 1, Japan Society Of Mechanical Engineers, 1983, pp. 299–306.

[4] Y. C. Wu, L. C. Wen, Solar Thermal Power Systems Advanced Solar Thermal Technology Project: Solar receiver performance in the temperature range of 300 to 1300C, Technical Report, Jet Propulsion Lab., Pasadena, CA (USA), 01.10.1978. URL: `http://www.osti.gov/energycitations/product.biblio.jsp?osti\_id=6953298`.

[5] T. R. Tracey, F. A. Blake, C. Royere, C. T. Brown, One MWth solar cavity steam generator solar test program, in: C. Beach, E. Fordyce (Eds.), International Solar Energy Society, Annual Meeting, 1977, p. 21.

[6] L. L. Eyler, Predictions of convective losses from a solar cavity receiver, Technical Report, Battelle Pacific Northwest Labs., Richland, WA (USA), 01.01.1979.

[7] A. M. Clausing, An Analysis of Convective Losses from Cavity Solar Central Receivers, Solar Energy 27 (1981) 295–300.

[8] A. M. Clausing, Convective Losses from Cavity Solar Receivers - Comparisons between Analytical Predictions and Experimental Results, Journal of Solar Energy Engineering-Transactions of the ASME 105 (1983) 29–33.

[9] A. M. Clausing, J. M. Waldvogel, L. D. Lister, Natural Convection From Isothermal Cubical Cavities With a Variety of Side-Facing Apertures, Journal of Heat Transfer 109 (1987) 407.

[10] W. Stine, C. McDonald, Cavity receiver heat loss measurements, in: ISES World Congress, 1989.

[11] R. Y. Ma, Wind effects on convective heat loss from a cavity receiver for a parabolic concentrating solar collector, Technical Report SAND–92-7293, Sandia National Labs., Albuquerque, NM (United States) and California State Polytechnic Univ., Pomona, CA (United States). Dept. of Mechanical Engineering, 1993. URL: http://www.osti.gov/energycitations/product.biblio.jsp?osti_id=10192244. doi:10.2172/10192244.

[12] M. Prakash, S. B. Kedare, J. K. Nayak, Investigations on heat losses from a solar cavity receiver, Solar Energy 83 (2009) 157–170.

[13] J. B. Fang, J. J. Wei, X. W. Dong, Y. S. Wang, Thermal performance simulation of a solar cavity receiver under windy conditions, Solar Energy 85 (2011) 126–138.

[14] J.-S. Kim, P. Liovic, Y. C. S. Too, G. Hart, W. Stein, CFD Analysis of Heat Loss from 200kW Cavity Reactor, in: Proceedings Solarpaces 2011, 2011.

[15] OpenFOAM Foundation, ESI-OpenCFD releases OpenFOAM® 2.2.0, 2013. URL: http://www.openfoam.org/version2.2.0/.

[16] J. H. Ferziger, M. Perić, Computational methods for fluid dynamics, 3 ed., Springer, Berlin and and New York, 2002.

[17] S. Paitoonsurikarn, K. Lovegrove, G. Hughes, J. Pye, Numerical Investigation of Natural Convection Loss From Cavity Receivers in Solar Dish Applications, Journal of Solar Energy Engineering-Transactions of the ASME 133 (2011) 10.